Cleavage of semaphorin 4C interferes the neuroprotective effect of semaphorin 4C/Plexin B2 pathway on experimental intracerebral hemorrhage in rats

Xiang Xu
First Affiliated Hospital of Soochow University
Xiang Li
First Affiliated Hospital of Soochow University
Haiying Li
First Affiliated Hospital of Soochow University
Haitao Shen
First Affiliated Hospital of Soochow University
Wanchun You
First Affiliated Hospital of Soochow University
Gang Chen (nju_neurosurgery@163.com)
First Affiliated Hospital of Soochow University https://orcid.org/0000-0002-0758-1907

Research

Keywords: Semaphorin 4C, plexin B2, intracerebral hemorrhage, apoptosis, neuronal injury

Posted Date: September 22nd, 2022

DOI: https://doi.org/10.21203/rs.3.rs-1869123/v1

Abstract

Semaphorin 4C (SEMA4C) and its cognate receptor Plexin B2 are important regulators of axon guidance and are involved in many neurological diseases, in which SEMA4C acts not only as a ligand ("forward" mode) but also as a signaling receptor ("reverse" mode). However, the role of SEMA4C/Plexin B2 in intracerebral hemorrhage (ICH) remains unclear. In this study, ICH in adult male Sprague-Dawley rats was induced by autologous blood injection in the right basal ganglia.In vitro, cultured primary neurons were subjected to OxyHb to imitate ICH injury. Recombinant SEMA4C (rSEMA4C) and overexpressing lentiviruses encoding full-length SEMA4C or secretory SEMA4C (sSEMA4C) were administered to rats by intraventricular injection. First, we found that elevated levels of sSEMA4C in the cerebrospinal fluid (CSF) of clinical patients were associated with poor prognosis. And both SEMA4C and sSEMA4C were increased in brain tissue around hematoma after ICH in rats. Overexpression of SEMA4C could attenuate neuronal apoptosis, neurosis, and neurologic impairment after ICH. However, treatments with rSEMA4C or sSEMA4C overexpression exacerbated neuronal injury. In addition, when treated with SEMA4C overexpression, the forward mode downstream protein RhoA and the reverse mode downstream ID1/3 transcriptional factors of SEMA4C/Plexin B2 signaling were all activated. Nevertheless, when exposed to rSEMA4C or sSEMA4C overexpression, only the forward mode was activated. Thus, sSEMA4C may be a novel molecular biomarker to predict the prognosis of patients with ICH, and the prevention of SEMA4C cleavage is expected to be a promising therapeutic target.

Introduction

Stroke is the second most common cause of death and the third leading cause of disability worldwide [1]. Although intracerebral hemorrhage (ICH) just accounts for approximately 10–15% of all strokes [2]. Patients who suffer from ICH are more likely to die or be permanently disabled than those who suffer from ischemic strokes [3]. In addition, the incidence of ICH among Asians is higher than most other racial groups [4]. Despite an abundance of research, there have been limited breakthroughs in the management of ICH.

Semaphorins are a large family including membrane-bound and secretory proteins, which were initially discovered as regulators of axonal guidance and cell migration in neurodevelopment [5, 6]. In addition, semaphorin family members have also been reported to mediate remyelination [7], the integrality of the blood brain barrier [8], and synaptic plasticity [9] in the mature nervous system. There are about 20 semaphorins, which are grouped into eight classes based on their structural features. Semaphorin 4C (SEMA4C) is a membrane-bound protein that is mainly expressed on cerebral cortical neurons [10]. Membrane-bound SEMA4C (mSEMA4C) has been reported to be cleaved by matrix metalloproteinases (MMPs) to release a secretory form in tumor-associated lymphatic endothelial cells (LECs). Secretory SEMA4C (sSEMA4C) promotes the proliferation and migration of tumor cells by combining with Plexin B2 [11]. Previous studies have indicated that SEMA4C elicits functions in neurogenesis induced by cerebral ischemia [12].

Plexin B2 is a high-affinity receptor of SEMA4C [13]. All semaohorins act through the intracellular domain of the plexins. Through protein interactions with Plexin B2, SEMA4C can direct activate RhoA activity, which is known as the “forward” signaling pathway [14]. Our previous study had demonstrated that miR-133b exhibited a neuroprotective effect following ICH by suppressing RhoA activity [15]. Furthermore, transmembrane semaphorins can also act as ligands by a “reverse” signaling model [16]. A recent study found that SEMA4C can initiate a signaling cascade through their own cytoplasmic domains, which leads to the increased abundance of inhibitor of differentiation 1 (ID1) and inhibitor of differentiation 3 (ID3) transcriptional factors [17]. In small cell lung cancer, increased expression of ID1 and ID3 can promote maliganant progression through suppressing apoptosis [18]. However, the SEMA4C/Plexin B2 forward and reverse signaling pathways after ICH have been poorly investigated so far, and their functions remain unknown.

Our study provides further understanding of the functional relevance of the SEMA4C/Plexin B2 bidirectional signaling pathway after ICH. We found that sSEMA4C protein levels were higher in the cerebrospinal fluid (CSF) of patients with ICH, which was associated with poor prognosis. mSEMA4C was upregulated after ICH, and the protein level of sSEMA4C cut by MMP also increased. In addition, following transfection with lentiviruses encoding SEMA4C, both the forward and reverse SEMA4C/Plexin B2 signaling modes were activated, which attenuated neuronal apoptosis. While treatment with recombinant SEMA4C (rSEMA4C) or sSEMA4C overexpressing, only the forward SEMA4C/Plexin B2 signaling cascade could be detected and neuronal injury was exacerbated. These findings may account for the observed correlation between elevated sSEMA4C levels and poor prognosis and provide new ideas for the treatment of ICH.

Materials And Methods

Animals

The experimental designs of this study were approved by the institutional Animal Care and Use Committee of the First Affiliated Hospital of Soochow University, Suzhou, Jiangsu Province. We performed all animal procedures strictly according to the National Institutes of Health guidelines. The results of animal experiments were reported according to AARIVE (Animal Research: Reporting in vivo Experiments). Male Sprague-Dawley (SD) rats (weight: 250–300 g) were purchased from the Experimental Animal Center of the Chinese Academy of Sciences (Shanghai, China). All rats were housed in the applicable environment under regular light alternates with dark (12h/12h) cycle and unlimited access to water and food. We minimized the numbers of rats that were used for the experiments as much as possible.

CSF collection

The experimental designs of this study were approved by the Medical Ethics Committee of the First Affiliated Hospital of Soochow University, Suzhou, Jiangsu Province. 500μl CSF were collected from 10 patients with normal pressure hydrocephalus who need routine lumbar puncture drainage test after

admission. Moreover, 500μl CSF from patients with ICH were obtained during the operation. During the removal of the hematoma via the lateral fissure approach, the outflow of CSF was quickly absorbed by a syringe. The specific information of patients is shown in Table S1. [19].

Establishment of the experimental ICH model in rats

The experimental ICH model was conducted in vivo by injection of autologous-arterial blood [3]. Briefly, rats were anaesthetized by inhalation of 5% isoflurane initially. After successful anesthetization, SD rats were fixed in a prone position on the stereotaxic frame (Zhenghua Biological Equipment Co. Ltd., Anhui, China). The periosteum was exposed after the median scalp was incised under aseptic conditions; we drilled a hole above the right basal ganglia (3.5 mm to the right and 0.2 mm posterior to the bregma). A total of 150 μl autologous rat blood was obtained from the caudal artery, then a microsyringe equipped with 100 μl autologous-arterial blood was slowly inserted to a depth of 5.5 mm and injected (20 μl/min) into the right basal ganglia. The position of the needle was maintained after the injection was completed. Bone wax was used to burr the hole and the skin incision was sutured. The heart rate of the animal was monitored and the body temperature was maintained at 37 ± 1°C during the surgical procedure. The rats in the sham group underwent the same procedure, with the exception that an equal volume of saline solution was injected instead of blood.

Experimental design

This experiment was divided into six parts (Figure S1). In experiment 1, we collected CSF from 10 patients with normal pressure hydrocephalus and 16 patients with ICH. All of the samples were detected by ELISA. Experiment 2 was performed to further investigate the changes in the protein level of SEMA4C and Plexin B2 after ICH. Additionally, the relationship between SEMA4C and Plexin B2 after ICH were verified by co-immunoprecipitation (Co-IP) testing. To evaluate the effect of recombinant SEMA4C after ICH, Rats were randomly divided into five groups in experiment 3: sham, ICH + vehicle (phosphate buffered saline [PBS]), ICH + rSEMA4C (0.15 μg/kg), ICH + rSEMA4C (0.5 μg/kg), and ICH + rSEMA4C (1.5 μg/kg). rSEMA4C was administered by intraventricular injection at 1 h post-ICH. Based on the outcomes, a dose of 0.5 μg/kg was found to be optimal for the following experiments.

Based on the experiments above, the following experiments exploited the time period at 24 h after ICH. In experiment 4 and 5, rats were randomly average divided into seven groups: sham, ICH, ICH + Vehicle, ICH + rSEMA4C, ICH + LV-Con, ICH + LV-SEMA4C, and ICH + LV-SEMA4C-secr. At 24 h after ICH,,rats were uesed for terminal deoxynucleotidy1 transferase-mediated dUTP nick-end labeling (TUNEL) staining, fluoro- Jade B (FJB) staining, and ethological testing. In experiment 6, primary-cultured neurons were used; enriched neurons were exposed to oxyhemoglobin (OxyHb) to simulate ICH in vitro. Neurons were divided into five groups as follows: Control, OxyHb, OxyHb + LV-Con, OxyHb + LV-SEMA4C, and OxyHb + LV-SEMA4C-secr. After 24 h of OxyHb exposure, the cells were collected for immunofluorescent staining, GLISA, and live-death cell-viability assay. The sum mary of experiment groups and mortality rate are showed in Table S2.

ELISA

The human CSF samples were collected to detect the levels of sSEMA4C using specific ELISA kits (Fusheng Industril, Shanghai, China) according to the manufacturers' instructions.

Primary cortical neurons cultures

Cortical neurons were isolated from primary rat embryos and cultured as described previously [20]. Briefly, cortical tissues of 18th-day rat embryos were isolated from the whole brain after removing the meninges and blood vessels. Next, 0.25% trypsin-EDTA solution was used to digest the cortical tissues for 5–8 min at 37°C. Then, the supernatant was centrifuged at 1500 r/min for 5 min, followed by filtration of the brain suspension. Dissociated neurons were plated onto 6- or 12-well plates (Corning, USA) precoated with 0.1 mg/ml poly-D-lysine (Sigma, USA), cultured in Neurobasal medium supplemented with 2% B-27 and 0.5 mM GlutaMAX TM- I (all Gibco, Carlsbad, CA, USA), and maintained at 37°C under humidified conditions and 5% CO_2. Half of the medium was changed every two days. Based on previous experience [21], Oxygen hemoglobin (OxyHb) was used to stimulate ICH injury in vitro, primary cortical neurons were incubated with OxyHb (20 μM) at 37 °C and 5% CO2 for 24 h.

Antibodies and drugs

Anti-SEMA4C antibody (sc-136445) and Anti-ID-3 antibody (sc-56712) were from Santa Cruz Biotechnology. Rb pAb to NeuN (ab104225), Anti-ID-1 antibody (ab230679), and Recombinant human semaphorin 4c (ab162889) were purchased from Abcam. Anti-Plexin B2 antibody (Fnab06545) was from FineTest. Cleaved-caspase-3 antibody (BF0711), β-tubulin antibody (AF7011), and GAPDH antibody (AF7021) were from Affinity Biosciences. Protein A/G immunoprecipitated magnetic beads (B23202) were from Bimake. Normal rabbit IgG (2729) was from Cell Signaling Technology. RhoA G-LISA Activation Assay Kit (Colorimetric Format) (BK124) was from Cytoskeleton, Inc. Human semaphorin 4c ELISA kits (A100745-96) were from Shanghai Fusheng Industrial Co., Ltd. GM6001 (A13320) was purchased from AdooQ BioScience. Secondary antibodies for western blot analysis, including goat anti-mouse IgGHRP (sc-2005) and goat anti-rabbit IgG-HRP (sc-2004), were obtained from Santa Cruz Biotechnology. Secondary antibodies for immunofluorescence analysis, including Alexa Fluor-488 donkey anti-rabbit IgG antibody (A21206), Alexa Fluor-555 donkey anti-rabbit IgG antibody (A31572), and Alexa Fluor-555 donkey anti-mouse IgG antibody (A31570), were purchased from Invitrogen.

Lentiviral transduction

Full-length rat SEMA4C cDNA was obtained from www.uniprot.org:D4A9J3, and its mutant, containing secretory extracellular domain (SEMA4C-secr), was generated by GeneChem Company (China). The sequence elements of lentiviral vector were Ubi-MCS-3FLAG-SV40-puromycin (Table S3). The titer of LV-SEMA4C was 2.8×10^8 TU/ml and the titer of LV-SEMA4C-secr was 1×10^8 TU/ml. In vivo, intraventricular injection of lentivirus was conducted according to the methods outlined in a previous study [22]. Briefly, 10 days before ICH surgery, SD rats were fixed on a stereotaxic apparatus after anesthesia. The amount

of lentivirus injected in each rat was 5×10^5 TU. A left side hole was drilled 1.5 mm lateral and 1.1 mm posterior to the bregma, and lentivirus was slowly infused into the lateral ventricle (3.5-mm depth) at a speed of 0.5 μl/min. The microsyringe was withdrawn slowly 5 min after injection to avoid reflux. The burr hole was closed with bone wax. In vitro, primary neurons were transduced with moderate LV (multiplicity of infection [MOI] = 10), and addition of 20 μl HA (HitransG A, GeneChem Co., Shanghai) enhanced the transduction solution 5–7 days after successful extraction.

Drug administration

According to a previous study [23], GM6001 (a broad-spectrum MMP inhibitor) was dissolved in DMSO and diluted to the final concentration with 0.9% normal saline. GM6001 (50 mg/kg) or equal volume of vehicle was administered intraperitoneally 2 h after the induction of ICH. In vivo, recombinant human semaphorin 4C was injected into the left lateral ventricles 1 h after ICH induction. The intracerebroventricular injection was performed as described above. Three doses of recombinant human semaphorin 4C were tested (0.15 μg/kg, 0.5 μg/kg, and 1.5 μg/kg).

Western blot analysis

The brains of rats were isolated after lavage with PBS, and the cerebral cortex surrounding the hematoma was collected. Cortical tissue was mechanically lysed in a lysis buffer. The supernatant was discarded after the lysed cortical tissue was centrifuged (12,000 r/min, 4°C, 5min). The final protein concentration was measured using the BCA protein Assay Kit (Beyotime, China). Molecular weight makers (Thermo Fisher Scientific, Waltham, MA, USA) and an equal volume of protein samples were loaded on sodium dodecyl sulfate (SDS)-polyacrylamide gel, separated, and electro-transferred onto a nitrocellulose membrane (Millipore Corporation, Billerica, MA, USA). Then, the membrane was blocked in 5% bovine serum albumin (BSA) blocking buffer for 1 h at room temperature. Subsequently, the membrane was incubated overnight at 4°C with primary antibodies against SEMA4C, Plexin B2, ID1, ID3, and cleaved caspase-3. Subsequently, the membrane was incubated with the corresponding HPR-conjugated secondary antibodies for 1 h at room temperature. After washing three times with PBST, the protein bands were detected by an enhanced chemiluminescence (ECL) kit (Beyotime, China). ImageJ software (NIH, Bethesda, MA, USA) was used to analyze the density of the protein bands. β-tubulin or GAPDH functioned as a loading control.

Co-immunoprecipitation （Co-IP）

The sample of brain tissue was prepared as described for western blotting. Briefly, brain samples were ground in a cell lysis buffer (Beyotime, China) and centrifuged to obtain the supernatant. Each supernatant was rotated for 1 h at 4°C after addition of Protein A/G immunoprecipitated magnetic beads. The samples were centrifuged again, and the supernatant was collected. Anti-Plexin B2 antibody or normal IgG were combined into the supernatant and rotated overnight at 4°C. Thereafter, the beads were added and rotated for a further 4 h at 4°C. The protein-antibody-bead mixture was centrifuged and the

supernatant was removed. Then, the precipitate was denatured with the SDS loading buffer. Finally, the protein was further detected by western blotting.

TdT-mediated dUTP-biotin nick end labeling (TUNEL) staining

TUNEL staining was utilized to quantity cellular apoptosis around the hematoma according to the manufacturer's protocol. The TUNEL-positive cells in the area of interest were observed and analyzed using a fluorescence microscope (OLYMPUS BX50/BX-FLA/DP70; Olympus Co., Japan). An observer who was blinded to the group allocation was responsible for counting and analyzing the positive cells.

Fluoro-Jade B (FJB) staining

FJB is a classic stain that is used to detect degenerated cells in brain tissue. The brain sections were dewaxed and rehydrated, and then transferred to a 0.06% $KMnO_4$ solution in the dark for 15 min at room temperature. After washing three times, the slides were immersed in 0.0004% FJB working solution for 20 min. Subsequently, the slides were incubated in an incubator (50–60°C) for 30min, and enveloped with neutral resins. Finally, the sections were surveyed by a fluorescence microscope.

Immunofluorescence analysis

In the in vivo experiments, the brain tissue was fixed, embedded, and cut into 4-μm sections. In the in vitro experiments, cultured neurons were fixed. The specific methods have been described previously [24]. Laconically, sections and cells were incubated with primary antibodies and then homologous secondary antibodies. The nuclei were stained with DAPI mounting medium. Lastly, a fluorescence microscope was used for observing the sections and cells. Quantitative analysis was performed by observers who were blinded to the group allocation.

Cell-viability assay

A cell-viability assay (Invitrogen, USA) was performed according to the manufacturer's instructions. Briefly, green dots (membrane-permeant calcein AM) indicated live cells and red dots (fluorescent ethidium homodimer-1) represented dead cells. The cells in three random fields were counted by a blinded observer. The experiments were repeated three times.

RhoA activity assay

GTP-bound RhoA was measured using G-LISA Activation Assay Kits (Cytoskeleton), according to the method reported previously [25, 26]. Following stimulation, the cells were washed three times with cold PBS and lysed with lysis buffer for 15 min on ice. The mixture was centrifuged at 10000 × g for 1 min at 4°C. Then, the supernatants were aliquoted, snap-frozen in liquid nitrogen, and stored at −80°C. GTP-bound RhoA activity was evaluated following the manufacturer's instructions.

Brain water content

Rats were administered intraperitoneally with 4% chloral hydrate 24 h after ICH. The total brain tissue was removed immediately, and the brain was separated into two hemispheres symmetrically; each hemisphere was further divided into two parts containing the cortex and basal ganglia. The final samples consisted of five parts: the ipsilateral basal ganglia (Ipsi-BG), the ipsilateral cortex (Ipsi-CX), the contralateral basal ganglia (Cont-BG), the contralateral cortex (Cont-CX), and the cerebellum (CB). The wet samples were weighed and recorded immediately. Then, the samples were moved to a thermostatic drier at 100°C for 72 h. The dried samples were also weighed and recorded, and the value of (wet weight – dry weight)/ (wet weight) × 100% was calculated.

Modified Garcia score test

The modified Garcia score was recorded as previously described [27]. The score consists of seven individual tests that assess spontaneous activity, axial sensation, vibrissae proprioception, symmetry of limb movement, lateral turning, forelimb walking, and climbing. Each subtest was given a score ranging from 0 to 3, with a maximum neurological score of 21.

Adhesive-removal test

The adhesive-removal test was used to access motor coordination and sensory function of the rat forelimbs after ICH [28]. The rats were placed in a cage for a few min to become familiar with the testing environment, and then a 9-mm circular sticker was attached to the palms of the bilateral forelimbs of the rats. The rats received training, which involved removing both stickers from the forepaws, for three days before ICH. After the surgery, the test was performed on days 1, 7, 14, and 20, and the time was recorded by two blinded observers.

Rotarod test

The rotarod test was used to evaluate the motor function of rats [29, 30]. The rats were initially placed onto the (10-cm diameter) (ZH-300B, Anhui Zhenghua Biological Equipment Co. Ltd., Anhui, China). The initial speed was 5 rpm, and was increased by 0.5 rpm per second. The rotarod cylinder stopped automatically at 1 min. Each rat received for three days, three times a day. The time at which the rats dropped or gripped the rotarod spindle and spun for two consecutive revolutions was recorded. After ICH surgery, the test was performed on days 1, 7, 14, and 20. Two blinded researchers were responsible for data recording.

Morris water maze

Morris water maze tests (swim distance and escape latency) were performed to access spatial cognitive functional deficits on days 21 to 25 after ICH. The Morris water maze test probe quadrant duration was measured on day 25 after ICH [31]. A round pool (180-cm diameter) filled with opaque water fell into four quadrants. A platform (10-cm diameter) was submerged in the pool at a depth of 1.5 cm and was set at a fixed position (the fourth quadrant). During the initial training phase, the rats were placed in the pool and given 60 s to find the fixed platform. Rats that were unable to find the platform in the stipulated time were

induced to the platform and allowed to stay for 10 s to intensify their learning and memory. ICH surgery was performed after five days of training. Escape latency (EL) referred to the time that the rats took to reach the target platform from the starting point. During the formal experiments, the rats were placed in the second quadrant and allowed to find the platform. Both ELs and swimming distances were recorded on days 21 to 25; then, on the 26th day after the above experiments, the platform was removed. The rats were placed in the second quadrant again, and the number of times that the rats swam through the previous platform within 60 s was recorded to evaluate the spatial memory. The swimming speed of each test was recorded to assess the general locomotor functions of rats. The room temperature was maintained at 25 ± 2°C, and the water temperature was maintained at 20 ± 2°C during the entire process.

Statistical analysis

All data were analyzed by GraphPad Prism 8.0 software (GraphPad, San Diego, CA, USA) and presented as the mean ± SD. All data were tested for normality, and two-sided unpaired Student's t-test was used to compare the two groups. The correlation between two variables was determined by Pearson's correlation test. A one- or two-way ANOVA was adopted to compare differences between groups. Tukey's multiple comparisons have been conducted for multiple testing. P-values < 0.05 were considered to indicate a statistically significant difference. Detailed statistics were shown in Table S4.

Results

Protein levels of SEMA4C and sSEMA4C increased after ICH

ELISA was used to identify the differences of sSEMA4C in CSF between ICH and non-ICH patients. The results showed that the protein level of sSEMA4C was higher in ICH patients than non-ICH patients (**Figure 1a**). Indeed, the protein level of sSEMA4C was negatively correlated with Glasgow outcome scale (GOS) prognosis score in patients who suffered ICH (**Figure 1b**). The ICH models of the SD rats were successfully established through injection of autologous-arterial blood (**Figure 1c**). western blotting was performed to detect the time course and spatial distribution of SEMA4C and Plexin B2 after ICH. The protein level of SEMA4C and Plexin B2 in the perihematomal cortex was assessed at 6 h, 12 h, 24 h, 48 h, 72h, and 168 h after induction of ICH in rats. The results demonstrated that, compared to the sham group, the protein levels of bothSEMA4C and sSEMA4C in brain tissue were significantly increased from 6 h to 72 h **(Figure 1d)**. However, there was no significant change in the protein level of Plexin B2 between the sham and ICH groups **(Figure 1e)**. Then brain tissue from the sham and ICH groups was chosen for CO-IP experiments. In the sham group, only SEMA4C could blind to Plexin B2. However. After ICH, the sSEMA4C protein level became higher, and both SEMA4C and sSEMA4C could blind to Plexin B2. Meanwhile, the correlation between SEMA4C and Plexin B2 was significantly higher in the ICH-24 h group compared to the sham group (**Figure 1f**). **Recombinant semaphorin 4C exacerbates neurobehavioral deficits and brain edema at 24 h post-ICH**

To further clarify the relationship between sSEMA4C and ICH injury, recombinant semaphorin 4C (rSEMA4C) was injected into the left lateral ventricle at various doses (0.15 μg/kg, 0.5 μg/kg, and 1.5

μg/kg). rSEMA4C at 0.5 μg/kg and 1.5 μg/kg statistically exacerbated the neurobehavioral defect and the brain water content (BWC) in the right BG and CX was also increased compared with the ICH + vehicle group (**Figure 2a, b**). Hence, the dose of 0.5 μg/kg was chosen for the remainder of the in vivo experiments.

Cleavage of SEMA4C attenuates its neuroprotective effect after ICH

To identify the effects of different forms of SEMA4C on the neuronal injury of rats after ICH, we adopted a lentiviral vector to overexpress full-length rat SEMA4C and secretory SEMA4C (SEMA4C-secr) which contains a soluble extracellular domain that is used to represent sSEMA4C. The transfection efficiency of overexpression of SEMA4C and sSEMA4C in brain tissue was verified by western blot analysis. As shown in **Figure 3a**, transfection with LV-SEMA4C and LV-SEMA4C-secr significantly increased the expression of SEMA4C and sSEMA4C, respectively. TUNEL and FJB staining were conducted in brain sections at 24 h after ICH to further assess the influence of SEMA4C and sSEMA4C on neuronal apoptosis and necrosis, respectively. The number of TUNEL-positive neurons in the ICH group was greater than that in the sham group, while upregulating SEMA4C could significantly reverse this phenomenon **(Figure 3b and 3c)**. Nevertheless, treatment with rSEMA4C or LV-SEMA4C-secr after ICH made no significant difference to the extent of neuronal apoptosis. Interestingly, the index of FJB-positive cells in the cortex after ICH was statistically decreased in the LV-SEMA4C treatment group, while treatment with rSEMA4C or LV-SEMA4C-secr showed the opposite results with more neuronal necrosis after ICH **(Figure 3d and 3e)**.

Cleavage of SEMA4C affected the neurological recovery after ICH

The sensorimotor defect was corroborated by adhesive-removal and rotarod tests, the results demonstrated that SEMA4C overexpression improved sensorimotor function recovery after ICH **(Figure 4a)**. In the rotarod test, rats with SEMA4C overexpression stayed on the accelerated beam longer which suggested better recovery of motor coordination. However, treatment with rSEMA4C or LV-SEMA4C-secr aggravated sensorimotor deficits **(Figure 4b)**.

Morris water maze tests were conducted from 21 to 26 days post-ICH. Compared to the sham group, rats in the ICH group displayed severe disorders in cognitive behavior (**Figure 4c**). Upregulation of SEMA4C significantly improved the cognitive behavior of ICH-injured rats. But treatment with rSEMA4C or LV-SEMA4C-secr aggravate spatial cognitive impairment (**Figure 4d)**. The spatial probe test of water maze was performed to examine the memory of the rats at 26 days after ICH, when the platform was removed. Rats in the ICH + LV-SEMA4C group crossed the platform position more frequently than those in the ICH + LV-Con group. Conversely, the number of times that the rats treated with rSEMA4C or LV-SEMA4C-secr crossed the platform position was significantly lower **(Figure 4e)**. Moreover, rats from each group showed no statistical difference in swimming speed **(Figure 4f)**.

Overexpression of SEMA4C reduced neuronal death after OxyHb treatment in vitro

The transfection effect of overexpression of LV-SEMA4C and LV-SEMA4C-secr in cultured neurons was verified by immunofluorescent analysis. As shown in **Figure 5a**, the average value of transfection efficiency in each group was approximately 60%–70%. A cell-viability assay was preformed to investigate the neuronal injury in vitro. The result showed that upregulation of SEMA4C could significantly improve neuronal injury, while sSEMA4C overexpression caused more neuronal death **(Figure 5b)**.

Cleavage of SEMA4C reduces the neuroprotective effect of SEMA4C in brain injury after ICH

Next, we sought to investigate how different forms of SEMA4C impact neurological behavior after ICH. SEMA4C acting through the intracellular domain of Plexin B2 is known as classical forward signaling, which can influence the activity of Rho GTPases. Moreover, we aimed to determine whether SEMA4C reverse signaling participated in the recovery of ICH-induced injury. Upregulation of SEMA4C, but not rSEMA4C or SEMA4C-secr could enhance the activation of ID1 and ID3 transcriptional regulators (**Figure 6a and 6b**). At the same time, only overexpressing full-length transmembrane could inhibit the expression of cleaved caspase-3 after ICH, which is widely acknowledged as the terminal apoptosis protein (**Figure 6c**). To further evaluate the role of SEMA4C after ICH, an in vitro model was established using cultured neurons and OxyHb. The GTP-bound RhoA level was detected by GLISA. Compared to the control group, RhoA activation was increased in neurons after OxyHb stimulation, and both overexpression of SEMA4C and SEMA4C-secr promoted the activation of GTP-bound RhoA (**Figure 6d**).

It has been reported that SEMA4C can be released in a secretory form by GM6001 on tumor-associated lymphatic cells [11]. We therefore analyzed whether this phenomenon existed in the brain after ICH. Using western blotting, we found that the release of sSEMA4C was significantly decreased by treatment with GM6001, while there was no significant change in the protein level of SEMA4C (**Figure 6e**).

Discussion

ICH is the most common hemorrhagic stroke subtype, and has poor outcomes. There is currently no effective interventional surgical or pharmacologic therapy for decreasing mortality or morbidity from ICH [32]. Therefore, there has been growing interest in determining effective targets for treating ICH.

Molecular biomarkers play a crucial role in the diagnosis and treatment of many diseases, such as tau protein in Alzheimer's disease (AD). However, the features of the blood brain barrier (BBB) and its potential for injury make it difficult to detect and use molecular biomarkers in the central nervous system (CNS). Previous studies have shown that the enhancement of CSF s100β [33], creatinine kinase brain isoenzyme (CKBB) [34], and neurofilaments (NFL) [35] were associated with poor outcomes after cardiac arrest. Elevated serum s100β is known to be associated with poor ICH outcomes in the acute phase [36, 37]. Moreover, neurofilament protein is released into the extracellular space following axonal damage, and has been found in many CNS diseases, such as stroke, AD, and spinal cord injury. In this study, we found elevated sSEMA4C protein levels in patients with ICH, which correlated with poor GOS, which may provide a novel avenue to predict the prognosis of ICH.

Recently, SEMA4C has been extensively studied in various pathological conditions, such as tumor progression [38, 39] and immune response [40]. Moreover, Wu et al. found that SEMA4C plays an important role in neurogenesis after ischemia-perfusion injury [12]. Simonetti et al. reported that SEMA4C mediated fear-induced structural plasticity by facilitating dendritic ramifications and regulating synaptic density in the adult hippocampus [14]. However, no previous studies have investigated the role of SEMA4C in ICH-induced brain injury. Therefore, in this study, we focused on the expression of SEMA4C after ICH and explored its possible functions and mechanisms. Our research demonstrated that the expression of SEMA4C increased after ICH, and that overexpression of SEMA4C could alleviate neuronal apoptosis and neurosis, as well as to neurological damage after ICH.

Class 4 semaphorins are transmembrane molecules, which can engage short-range cell-to-cell interactions with neighboring cells. In many cases, their extracellular moiety can be cleaved in soluble form and function as a secreted signal. For instance, Semaphorin 4D (SEMA4D) can be shed in secretory SEMA4D, which promotes sprouting and angiogenesis in endothelial cells [41]. In addition, some semaphorin family molecules show different biological properties between their membrane and soluble forms. Mumblat et al. reported that full-length SEMA3C could inhibit tumor angiogenesis and lymphatic metastasis, while cleaved SEMA3C (p65-SEMA3C) is a pro-tumorigenic factor [42]. Our results also showed that full-length SEMA4C and sSEMA4C existed in brain tissue, and that both were elevated after ICH. Moreover, the MMP inhibitor GM6001 could block SEMA4C release sSEMA4C following ICH. Through different means of intervention, SEMA4C showed neuroprotective roles, while sSEMA4C had the opposite effect in ICH-induced brain injury. MMPs are involved in inflammation, BBB disruption, edema, and neuronal death after ICH [43]. GM6001 has been reported to ameliorate brain injury after ICH by inhibiting MMPs [44]. The possible mechanism of neuroprotection effect of GM6001 was briefly revealed in this study, which decreased SEMA4C release sSEMA4C.

The SEMA4C forward signaling pathway acts through the intracellular domain of Plexin B2, which elicits RhoA activation through interaction with RhoGEFs [45, 46]. RhoA belongs to the Ras/Rho family, and mediates cell motility by regulating actin and microtubules [17]. RhoA cycle between inactive GDP-bound and active GTP-bound states and function as molecular switches in signal transduction cascades. Our previous study had demonstrated that suppressing RhoA activity attenuate brain injury after ICH [15]. In addition, inhibiting the RhoA pathway could alleviate neurological deficits in cerebral ischemia/reperfusion injury [47], ICH-induced BBB injury [48], and traumatic brain injury [49]. We also found that overexpression of SEMA4C or SEMA4C-secr could increase the level of GTP-bound RhoA, resulting in further neuronal death in vitro after induction of ICH.

Although transmembrane semaphorins were initially found as ligands, recent studies have shown that transmembrane semaphorins also function as receptors, known as reverse signaling [10, 17]. Transmembrane semaphorins can elicit an activated cascade through their cytoplasmic domain. The cytoplasmic domain of many class 4 semaphorins possesses a PDZ domains at the C-terminus [50]. Semaphorin 4A (SEMA4A) and SEMA4D intracellular portions are reported to mediate cancer cell migration, through the recruitment of Rac1 regulatory molecules Scribble and T cell lymphoma invasion,

respectively [51, 52]. Moreover, blocking the PDZ domain-binding motif of SEMA4C has been shown to inhibit myogenic differentiation during muscle development [53]. Gurrapu et al. reported that the intracellular tail of SEMA4C interacted with transforming growth factor-β (TGF-β) surface receptors and initial a nonconventional signaling cascade, leading to the induction of ID1 and ID3 transcriptional regulators, resulting in invasive reprogramming in cancer cells, which was dependent on Plexin B2 [17]. These data suggest a putative role of SEMA4C reverse signaling. ID1 and ID3 expressed in the adult brain have been reported to negatively regulate the apoptotic process [54, 55]. Here, we report that the SEMA4C reverse signaling pathway was activated, and ID1 and ID3 were upregulated after ICH. This conclusion was further supported by the intervention of SEMA4C mutagenesis and soluble rSEMA4C in extracellular matrix.

Cell death is the major reason for brain injury following ICH. Both apoptotic and necrotic cells presented in the region surrounding the hematoma in patients and animal models after ICH [56]. Necrosis is characterized by disorganized cell death, whereas apoptosis can occur in a programmed manner. In this study, we found that the SEMA4C reverse pathway could inhibit neuronal apoptosis, while the SEMA4C forward pathway mainly accelerate neuronal necrosis. The underlying mechanisms of neuronal injury after ICH have not yet been elucidated. In this study, our data showed that increased sSEMA4C protein levels in the CSF of patients with ICH correlated with poor prognosis. Both the SEMA4C forward pathway and reverse pathway were activated after ICH, and the reverse signaling played a dominant role because of cleavage of SEMA4C. GM6001 could block SEMA4C to release sSEMA4C. In conclusion, SEMA4C may be a therapeutic target for ICH treatment andsSEMA4C is a potential molecular biomarker for predicting ICH progression (Fig. 7).

Conclusions

In summary, our findings demonstrate the mechanism of SEMA4C in ICH-induced neuronal injury. SEMA4C and Plexin B2 can interact in cis and trans after ICH; reverse signaling showed neuroprotective ability by elicit ID1 and ID3 which reduce cell apoptosis, while forward signaling depended on RhoA activity to increase necrosis. These findings emphasize the importance of SEMA4C after ICH, and may illuminate a new pharmacological mechanism for the treatment of ICH.

Abbreviations

SEMA4C, Semaphorin 4C; ICH, intracerebral hemorrhage; ICH, intracerebral hemorrhage; rSEMA4C, recombinant SEMA4C; sSEMA4C, secretory SEMA4C; CSF, cerebrospinal fluid; mSEMA4C, Membrane-bound SEMA4C; MMPs, matrix metalloproteinases; LECs, lymphatic endothelial cells; ID1, inhibitor of differentiation 1; ID3, inhibitor of differentiation 3; Co-IP, co-immunoprecipitation; PBS, phosphate buffered saline; OxyHb, oxyhemoglobin; MOI, multiplicity of infection; AD, Alzheimer’s disease; BBB, blood brain barrier; CNS, central nervous system; CKBB, creatinine kinase brain isoenzyme; NFL, neurofilaments; SEMA4D, Semaphorin 4D; TGF-β, transforming growth factor-β.

Declarations

Ethics approval and consent to participate

All animal experiments are strictly in accordance with the guideline of Soochow University institutional Animal Care and Use Committee.

Consent for publication

Not applicable.

Availability of data and materials

The datasets generated and/or analyzed during the current study are not publicly available due to the confidential policy of our hospital but are available from the corresponding author on reasonable request.

Competing interests

The authors have no relevant financial or non-financial interests to disclose.

Funding

This work was supported by the National Natural Science Foundation of China (No. 82101386), Natural Science Foundation of Jiangsu Province under Grant (No. BK20220096), and Postgraduate Research & Practice Innovation Program of Jiangsu Province (No. KYCX22_3234).

Authors' contributions

GC and WY participated in the design of this study. XX and XL performed the experiments and wrote the paper. HL and HS helped to design the analysis strategy and implement the analysis and constructive discussion. XX and XL conducted the literature review. GC and WY reviewed and edited the manuscript. All authors have critically revised the manuscript and approved the final version.

Acknowledgements

None

References

1. Owolabi MO, Thrift AG, Mahal A, Ishida M, Martins S, Johnson WD, Pandian J, Abd-Allah F, Yaria J, Phan HT, Roth G, Gall SL, Beare R, Phan TG, Mikulik R, Akinyemi RO, Norrving B, Brainin M, Feigin VL, Stroke Experts Collaboration G (2022) Primary stroke prevention worldwide: translating evidence into action. Lancet Public Health 7 (1):e74-e85. doi:10.1016/S2468-2667(21)00230-9

2. Schrag M and Kirshner H (2020) Management of Intracerebral Hemorrhage: JACC Focus Seminar. J Am Coll Cardiol 75:1819-1831. doi: 10.1016/j.jacc.2019.10.066
3. Shen F, Xu X, Yu Z, Li H, Shen H, Li X, Shen M and Chen G (2021) Rbfox-1 contributes to CaMKIIalpha expression and intracerebral hemorrhage-induced secondary brain injury via blocking micro-RNA-124. J Cereb Blood Flow Metab 41:530-545. doi: 10.1177/0271678X20916860
4. Collaborators GBDCoD (2018) Global, regional, and national age-sex-specific mortality for 282 causes of death in 195 countries and territories, 1980-2017: a systematic analysis for the Global Burden of Disease Study 2017. Lancet 392:1736-1788. doi: 10.1016/S0140-6736(18)32203-7
5. Kolodkin AL, Matthes DJ and Goodman CS (1993) The semaphorin genes encode a family of transmembrane and secreted growth cone guidance molecules. Cell 75:1389-99. doi: 10.1016/0092-8674(93)90625-z
6. Luo Y, Raible D and Raper JA (1993) Collapsin: a protein in brain that induces the collapse and paralysis of neuronal growth cones. Cell 75:217-27. doi: 10.1016/0092-8674(93)80064-l
7. Biname F, Pham-Van LD, Spenle C, Jolivel V, Birmpili D, Meyer LA, Jacob L, Meyer L, Mensah-Nyagan AG, Po C, Van der Heyden M, Roussel G and Bagnard D (2019) Disruption of Sema3A/Plexin-A1 inhibitory signalling in oligodendrocytes as a therapeutic strategy to promote remyelination. EMBO Mol Med 11:e10378. doi: 10.15252/emmm.201910378
8. Yang M, Wang X, Fan Y, Chen Y, Sun D, Xu X, Wang J, Gu G, Peng R, Shen T, Liu X, Li F, Wang Y, Wang D, Rong H, Han Z, Gao X, Li Q, Fan K, Yuan Y and Zhang J (2019) Semaphorin 3A Contributes to Secondary Blood-Brain Barrier Damage After Traumatic Brain Injury. Front Cell Neurosci 13:117. doi: 10.3389/fncel.2019.00117
9. Orr BO, Fetter RD and Davis GW (2017) Retrograde semaphorin-plexin signalling drives homeostatic synaptic plasticity. Nature 550:109-113. doi: 10.1038/nature24017
10. Gurrapu S and Tamagnone L (2016) Transmembrane semaphorins: Multimodal signaling cues in development and cancer. Cell Adh Migr 10:675-691. doi: 10.1080/19336918.2016.1197479
11. Wei JC, Yang J, Liu D, Wu MF, Qiao L, Wang JN, Ma QF, Zeng Z, Ye SM, Guo ES, Jiang XF, You LY, Chen Y, Zhou L, Huang XY, Zhu T, Meng L, Zhou JF, Feng ZH, Ma D and Gao QL (2017) Tumor-associated Lymphatic Endothelial Cells Promote Lymphatic Metastasis By Highly Expressing and Secreting SEMA4C. Clin Cancer Res 23:214-224. doi: 10.1158/1078-0432.CCR-16-0741
12. Wu H, Fan J, Zhu L, Liu S, Wu Y, Zhao T, Wu Y, Ding X, Fan W and Fan M (2009) Sema4C expression in neural stem/progenitor cells and in adult neurogenesis induced by cerebral ischemia. J Mol Neurosci 39:27-39. doi: 10.1007/s12031-009-9177-8
13. Witherden DA, Watanabe M, Garijo O, Rieder SE, Sarkisyan G, Cronin SJ, Verdino P, Wilson IA, Kumanogoh A, Kikutani H, Teyton L, Fischer WH and Havran WL (2012) The CD100 receptor interacts with its plexin B2 ligand to regulate epidermal gammadelta T cell function. Immunity 37:314-25. doi: 10.1016/j.immuni.2012.05.026
14. Simonetti M, Paldy E, Njoo C, Bali KK, Worzfeld T, Pitzer C, Kuner T, Offermanns S, Mauceri D and Kuner R (2021) The impact of Semaphorin 4C/Plexin-B2 signaling on fear memory via remodeling of

neuronal and synaptic morphology. Mol Psychiatry 26:1376-1398. doi: 10.1038/s41380-019-0491-4

15. Shen H, Yao X, Li H, Li X, Zhang T, Sun Q, Ji C and Chen G (2018) Role of Exosomes Derived from miR-133b Modified MSCs in an Experimental Rat Model of Intracerebral Hemorrhage. J Mol Neurosci 64:421-430. doi: 10.1007/s12031-018-1041-2
16. Battistini C and Tamagnone L (2016) Transmembrane semaphorins, forward and reverse signaling: have a look both ways. Cell Mol Life Sci 73:1609-22. doi: 10.1007/s00018-016-2137-x
17. Gurrapu S, Franzolin G, Fard D, Accardo M, Medico E, Sarotto I, Sapino A, Isella C and Tamagnone L (2019) Reverse signaling by semaphorin 4C elicits SMAD1/5- and ID1/3-dependent invasive reprogramming in cancer cells. Sci Signal 12. doi: 10.1126/scisignal.aav2041
18. Chen D, Forootan SS, Gosney JR, Forootan FS, Ke Y (2014) Increased expression of Id1 and Id3 promotes tumorigenicity by enhancing angiogenesis and suppressing apoptosis in small cell lung cancer. Genes Cancer 5 (5-6):212-225. doi:10.18632/genesandcancer.20
19. Lehmann S, Dumurgier J, Ayrignac X, Marelli C, Alcolea D, Ormaechea JF, Thouvenot E, Delaby C, Hirtz C, Vialaret J, Ginestet N, Bouaziz-Amar E, Laplanche JL, Labauge P, Paquet C, Lleo A, Gabelle A, Alzheimer's Disease Neuroimaging I (2020) Cerebrospinal fluid A beta 1-40 peptides increase in Alzheimer's disease and are highly correlated with phospho-tau in control individuals. Alzheimers Res Ther 12 (1):123. doi:10.1186/s13195-020-00696-1
20. Wang Z, Zhou F, Dou Y, Tian X, Liu C, Li H, Shen H and Chen G (2018) Melatonin Alleviates Intracerebral Hemorrhage-Induced Secondary Brain Injury in Rats via Suppressing Apoptosis, Inflammation, Oxidative Stress, DNA Damage, and Mitochondria Injury. Transl Stroke Res 9:74-91. doi: 10.1007/s12975-017-0559-x
21. Zhang P, Wang T, Zhang D, Zhang Z, Yuan S, Zhang J, Cao J, Li H, Li X, Shen H, Chen G (2019) Exploration of MST1-Mediated Secondary Brain Injury Induced by Intracerebral Hemorrhage in Rats via Hippo Signaling Pathway. Translational stroke research 10 (6):729-743. doi:10.1007/s12975-019-00702-1
22. Hu L, Zhang H, Wang B, Ao Q and He Z (2020) MicroRNA-152 attenuates neuroinflammation in intracerebral hemorrhage by inhibiting thioredoxin interacting protein (TXNIP)-mediated NLRP3 inflammasome activation. Int Immunopharmacol 80:106141. doi: 10.1016/j.intimp.2019.106141
23. Chen W, Hartman R, Ayer R, Marcantonio S, Kamper J, Tang J and Zhang JH (2009) Matrix metalloproteinases inhibition provides neuroprotection against hypoxia-ischemia in the developing brain. J Neurochem 111:726-36. doi: 10.1111/j.1471-4159.2009.06362.x
24. Xue T, Sun Q, Zhang Y, Wu X, Shen H, Li X, Wu J, Li H, Wang Z and Chen G (2021) Phosphorylation at S548 as a Functional Switch of Sterile Alpha and TIR Motif-Containing 1 in Cerebral Ischemia/Reperfusion Injury in Rats. Mol Neurobiol 58:453-469. doi: 10.1007/s12035-020-02132-9
25. Zhang Y, Yan J, Xu H, Yang Y, Li W, Wu H and Liu C (2018) Extremely low frequency electromagnetic fields promote mesenchymal stem cell migration by increasing intracellular Ca(2+) and activating the FAK/Rho GTPases signaling pathways in vitro. Stem Cell Res Ther 9:143. doi: 10.1186/s13287-018-0883-4

26. Lopez-Posadas R, Fastancz P, Martinez-Sanchez LDC, Panteleev-Ivlev J, Thonn V, Kisseleva T, Becker LS, Schulz-Kuhnt A, Zundler S, Wirtz S, Atreya R, Carle B, Friedrich O, Schurmann S, Waldner MJ, Neufert C, Brakebusch CH, Bergo MO, Neurath MF and Atreya I (2019) Inhibiting PGGT1B Disrupts Function of RHOA, Resulting in T-cell Expression of Integrin alpha4beta7 and Development of Colitis in Mice. Gastroenterology 157:1293-1309. doi: 10.1053/j.gastro.2019.07.007
27. Chen S, Zhao L, Sherchan P, Ding Y, Yu J, Nowrangi D, Tang J, Xia Y and Zhang JH (2018) Activation of melanocortin receptor 4 with RO27-3225 attenuates neuroinflammation through AMPK/JNK/p38 MAPK pathway after intracerebral hemorrhage in mice. J Neuroinflammation 15:106. doi: 10.1186/s12974-018-1140-6
28. Chau MJ, Deveau TC, Gu X, Kim YS, Xu Y, Yu SP and Wei L (2018) Delayed and repeated intranasal delivery of bone marrow stromal cells increases regeneration and functional recovery after ischemic stroke in mice. BMC Neurosci 19:20. doi: 10.1186/s12868-018-0418-z
29. Chen J, Li Y, Wang L, Zhang Z, Lu D, Lu M and Chopp M (2001) Therapeutic benefit of intravenous administration of bone marrow stromal cells after cerebral ischemia in rats. Stroke 32:1005-11. doi: 10.1161/01.str.32.4.1005
30. Chan SJ, Zhao H, Hayakawa K, Chai C, Tan CT, Huang J, Tao R, Hamanaka G, Arumugam TV, Lo EH, Yu VCK and Wong PH (2019) Modulator of apoptosis-1 is a potential therapeutic target in acute ischemic injury. J Cereb Blood Flow Metab 39:2406-2418. doi: 10.1177/0271678X18794839
31. Yan J, Zuo G, Sherchan P, Huang L, Ocak U, Xu W, Travis ZD, Wang W, Zhang JH and Tang J (2020) CCR1 Activation Promotes Neuroinflammation Through CCR1/TPR1/ERK1/2 Signaling Pathway After Intracerebral Hemorrhage in Mice. Neurotherapeutics 17:1170-1183. doi: 10.1007/s13311-019-00821-5
32. Wilkinson DA, Pandey AS, Thompson BG, Keep RF, Hua Y and Xi G (2018) Injury mechanisms in acute intracerebral hemorrhage. Neuropharmacology 134:240-248. doi: 10.1016/j.neuropharm.2017.09.033
33. Oda Y, Tsuruta R, Fujita M, Kaneda K, Kawamura Y, Izumi T, Kasaoka S, Maruyama I and Maekawa T (2012) Prediction of the neurological outcome with intrathecal high mobility group box 1 and S100B in cardiac arrest victims: a pilot study. Resuscitation 83:1006-12. doi: 10.1016/j.resuscitation.2012.01.030
34. Sherman AL, Tirschwell DL, Micklesen PJ, Longstreth WT, Jr. and Robinson LR (2000) Somatosensory potentials, CSF creatine kinase BB activity, and awakening after cardiac arrest. Neurology 54:889-94. doi: 10.1212/wnl.54.4.889
35. Rosen H, Karlsson JE and Rosengren L (2004) CSF levels of neurofilament is a valuable predictor of long-term outcome after cardiac arrest. J Neurol Sci 221:19-24. doi: 10.1016/j.jns.2004.03.003
36. Hu YY, Dong XQ, Yu WH and Zhang ZY (2010) Change in plasma S100B level after acute spontaneous basal ganglia hemorrhage. Shock 33:134-40. doi: 10.1097/SHK.0b013e3181ad5c88
37. James ML, Blessing R, Phillips-Bute BG, Bennett E and Laskowitz DT (2009) S100B and brain natriuretic peptide predict functional neurological outcome after intracerebral haemorrhage.

Biomarkers 14:388-94. doi: 10.1080/13547500903015784

38. Jing L, Bo W, Yourong F, Tian W, Shixuan W and Mingfu W (2019) Sema4C mediates EMT inducing chemotherapeutic resistance of miR-31-3p in cervical cancer cells. Sci Rep 9:17727. doi: 10.1038/s41598-019-54177-z
39. Smeester BA, Slipek NJ, Pomeroy EJ, Bomberger HE, Shamsan GA, Peterson JJ, Crosby MR, Draper GM, Becklin KL, Rahrmann EP, McCarthy JB, Odde DJ, Wood DK, Largaespada DA and Moriarity BS (2020) SEMA4C is a novel target to limit osteosarcoma growth, progression, and metastasis. Oncogene 39:1049-1062. doi: 10.1038/s41388-019-1041-x
40. Yan H, Wu L, Shih C, Hou S, Shi J, Mao T, Chen W, Melvin B, Rigby RJ, Chen Y, Jiang H, Friedel RH, Vinuesa CG and Qi H (2017) Plexin B2 and Semaphorin 4C Guide T Cell Recruitment and Function in the Germinal Center. Cell Rep 19:995-1007. doi: 10.1016/j.celrep.2017.04.022
41. Conrotto P, Valdembri D, Corso S, Serini G, Tamagnone L, Comoglio PM, Bussolino F and Giordano S (2005) Sema4D induces angiogenesis through Met recruitment by Plexin B1. Blood 105:4321-9. doi: 10.1182/blood-2004-07-2885
42. Mumblat Y, Kessler O, Ilan N and Neufeld G (2015) Full-Length Semaphorin-3C Is an Inhibitor of Tumor Lymphangiogenesis and Metastasis. Cancer Res 75:2177-86. doi: 10.1158/0008-5472.CAN-14-2464
43. Zhang X, Gu Y, Li P, Jiang A, Sheng X, Jin X, Shi Y and Li G (2019) Matrix Metalloproteases-Mediated Cleavage on beta-Dystroglycan May Play a Key Role in the Blood-Brain Barrier After Intracerebral Hemorrhage in Rats. Med Sci Monit 25:794-800. doi: 10.12659/MSM.908500
44. Lattanzi S, Di Napoli M, Ricci S, Divani AA (2020) Matrix Metalloproteinases in Acute Intracerebral Hemorrhage. Neurotherapeutics 17 (2):484-496. doi:10.1007/s13311-020-00839-0
45. McColl B, Garg R, Riou P, Riento K and Ridley AJ (2016) Rnd3-induced cell rounding requires interaction with Plexin-B2. J Cell Sci 129:4046-4056. doi: 10.1242/jcs.192211
46. Paldy E, Simonetti M, Worzfeld T, Bali KK, Vicuna L, Offermanns S and Kuner R (2017) Semaphorin 4C Plexin-B2 signaling in peripheral sensory neurons is pronociceptive in a model of inflammatory pain. Nat Commun 8:176. doi: 10.1038/s41467-017-00341-w
47. Gong P, Li R, Jia HY, Ma Z, Li XY, Dai XR and Luo SY (2020) Anfibatide Preserves Blood-Brain Barrier Integrity by Inhibiting TLR4/RhoA/ROCK Pathway After Cerebral Ischemia/Reperfusion Injury in Rat. J Mol Neurosci 70:71-83. doi: 10.1007/s12031-019-01402-z
48. Zhao H, Zhang X, Dai Z, Feng Y, Li Q, Zhang JH, Liu X, Chen Y and Feng H (2016) P2X7 Receptor Suppression Preserves Blood-Brain Barrier through Inhibiting RhoA Activation after Experimental Intracerebral Hemorrhage in Rats. Sci Rep 6:23286. doi: 10.1038/srep23286
49. Mulherkar S, Firozi K, Huang W, Uddin MD, Grill RJ, Costa-Mattioli M, Robertson C and Tolias KF (2017) RhoA-ROCK Inhibition Reverses Synaptic Remodeling and Motor and Cognitive Deficits Caused by Traumatic Brain Injury. Sci Rep 7:10689. doi: 10.1038/s41598-017-11113-3
50. Neufeld G, Mumblat Y, Smolkin T, Toledano S, Nir-Zvi I, Ziv K and Kessler O (2016) The semaphorins and their receptors as modulators of tumor progression. Drug Resist Updat 29:1-12. doi:

10.1016/j.drup.2016.08.001

51. Sun T, Yang L, Kaur H, Pestel J, Looso M, Nolte H, Krasel C, Heil D, Krishnan RK, Santoni MJ, Borg JP, Bunemann M, Offermanns S, Swiercz JM and Worzfeld T (2017) A reverse signaling pathway downstream of Sema4A controls cell migration via Scrib. J Cell Biol 216:199-215. doi: 10.1083/jcb.201602002
52. Zhou H, Kann MG, Mallory EK, Yang YH, Bugshan A, Binmadi NO and Basile JR (2017) Recruitment of Tiam1 to Semaphorin 4D Activates Rac and Enhances Proliferation, Invasion, and Metastasis in Oral Squamous Cell Carcinoma. Neoplasia 19:65-74. doi: 10.1016/j.neo.2016.12.004
53. Ko JA, Gondo T, Inagaki S and Inui M (2005) Requirement of the transmembrane semaphorin Sema4C for myogenic differentiation. FEBS Lett 579:2236-42. doi: 10.1016/j.febslet.2005.03.022
54. Diotel N, Beil T, Strahle U and Rastegar S (2015) Differential expression of id genes and their potential regulator znf238 in zebrafish adult neural progenitor cells and neurons suggests distinct functions in adult neurogenesis. Gene Expr Patterns 19:1-13. doi: 10.1016/j.gep.2015.05.004
55. Ling F, Kang B and Sun XH (2014) Id proteins: small molecules, mighty regulators. Curr Top Dev Biol 110:189-216. doi: 10.1016/B978-0-12-405943-6.00005-1
56. Zhang Z, Wu Y, Yuan S, Zhang P, Zhang J, Li H, Li X, Shen H, Wang Z and Chen G (2018) Glutathione peroxidase 4 participates in secondary brain injury through mediating ferroptosis in a rat model of intracerebral hemorrhage. Brain Res 1701:112-125. doi: 10.1016/j.brainres.2018.09.012

Figures

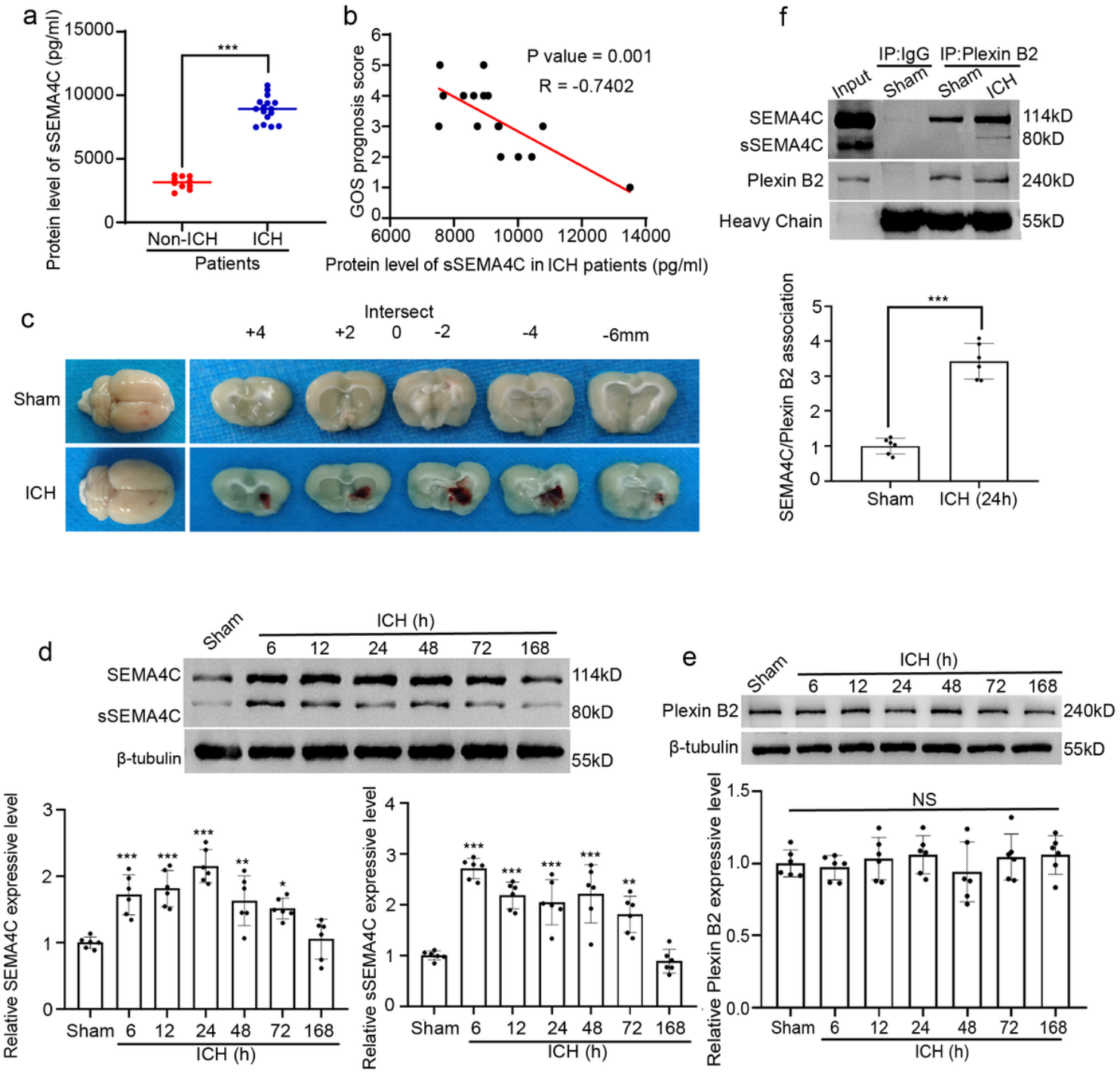

Figure 1

Protein level of SEMA4C and Plexin B2 in the CNS after ICH.

(a) The level of sSEMA4C in the CSF of patients in the non-ICH group (obtained from patients with normal pressure hydrocephalus, n = 10) and the ICH group (obtained from ICH patients within 3 days of onset, n = 16) (Non-ICH vs. ICH: P < 0.001). (b) Pearson correlation coefficient between sSEMA4C levels in the CSF of patients with ICH with GOS score (R = −0.7402, P = 0.001, n = 16). (c) Representative image of brain

sections. (d) Western blot analysis and quantification of the time course of the protein level of mSEMA4C (Sham vs. ICH 6h: P = 0.0007, Sham vs. ICH 12h: P = 0.0001, Sham vs. ICH 24h: P < 0.0001, Sham vs. ICH 48h: P = 0.0037, Sham vs. ICH 72h: P = 0.0281, Sham vs. ICH 168h: P = 0.9998) and sSEMA4C (Sham vs. ICH 6h: P < 0.0001, Sham vs. ICH 12h: P < 0.0001, Sham vs. ICH 24h: P = 0.0001, Sham vs. ICH 48h: P < 0.0001, Sham vs. ICH 72h: P = 0.0042, Sham vs. ICH 168h: P = 0.9973) in the brain tissue around the hematoma (n = 6). (e) Western blot analysis and quantification of the time course of the protein level of Plexin B2 in the brain tissue around the hematoma (Sham vs. ICH 6h: P = 0.9980, Sham vs. ICH 12h: P = 0.9958, Sham vs. ICH 24h: P = 0.9453, Sham vs. ICH 48h: P = 0.9503, Sham vs. ICH 72h: P = 0.9871, Sham vs. ICH 168h: P = 0.9506, n = 6). (f) CO-IP analysis and quantification of both mSEMA4C and sSEMA4C interacting with Plexin B2 in the brain tissue around the hematoma (ICH 24h vs. Sham: P < 0.0001, n = 6). In a, d, e and f, the data are presented as the mean ± SD; NS: No significant difference vs. sham group, *P < 0.05 vs. sham group, **P < 0.01 vs. sham group, ***P < 0.001 vs. sham group.

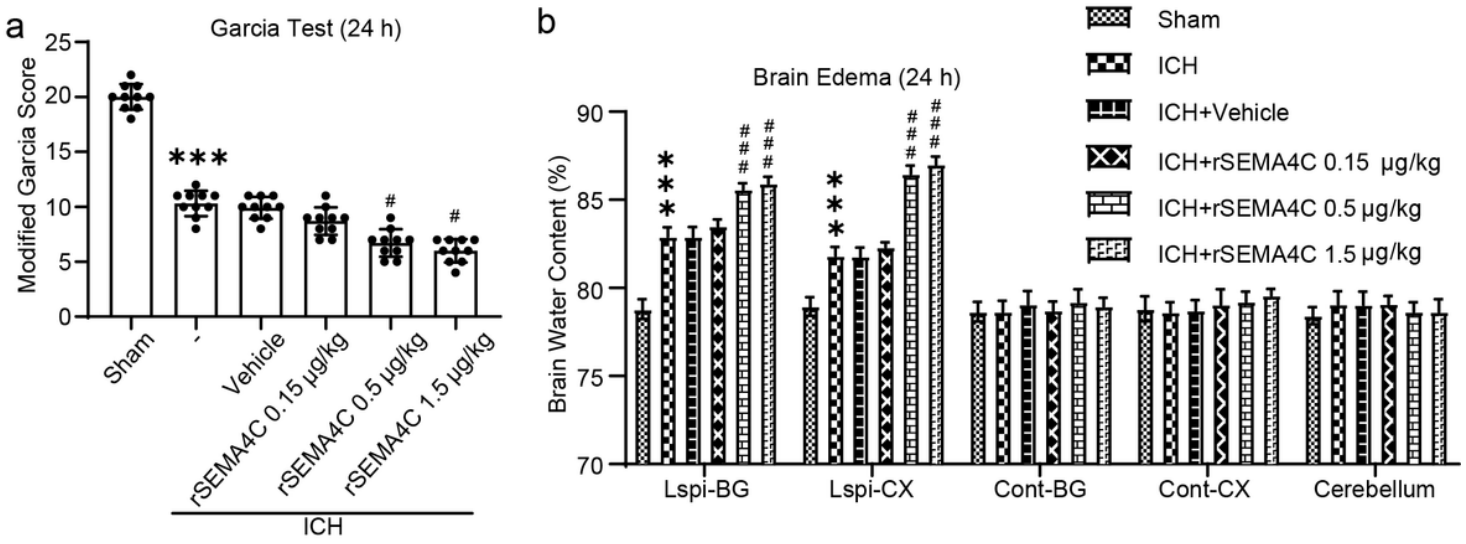

Figure 2

Effect of different doses of rSEMA4C on brain injury at 24 h.

(a) Modified Garcia test (Sham vs. ICH: P<0.0001, ICH vs. ICH+Vehicle: P=0.9669, ICH+Vehicle vs. ICH+ rSEMA4C 0.15μg/kg: p = 0.1783, ICH+Vehicle vs. ICH+ rSEMA4C 0.5μg/kg: p < 0.0001, ICH+Vehicle vs. ICH+ rSEMA4C 1.5μg/kg: p < 0.0001, n = 10). (b) Brain water content (Lspi-BG: Sham vs. ICH: P < 0.0001, ICH vs. ICH+Vehicle: P > 0.9999, ICH+Vehicle vs. ICH+ rSEMA4C 0.15μg/kg: p = 0.1815, ICH+Vehicle vs. ICH+ rSEMA4C 0.5μg/kg: p < 0.0001, ICH+Vehicle vs. ICH+ rSEMA4C 1.5μg/kg: p < 0.0001, Lspi-CX: Sham vs. ICH: P < 0.0001, ICH vs. ICH+Vehicle: P > 0.9999, ICH+Vehicle vs. ICH+ rSEMA4C 0.15μg/kg: p = 0.3318, ICH+Vehicle vs. ICH+ rSEMA4C 0.5μg/kg: p < 0.0001, ICH+Vehicle vs. ICH+ rSEMA4C 1.5μg/kg: p < 0.0001, Cont - BG: Sham vs. ICH: P >0.9999, ICH vs. ICH+Vehicle: P = 0.5553, ICH+Vehicle vs. ICH+ rSEMA4C 0.15μg/kg: p = 0.9996, ICH+Vehicle vs. ICH+ rSEMA4C 0.5μg/kg: p = 0.2495, ICH+Vehicle vs. ICH+ rSEMA4C 1.5μg/kg: p = 0.8413, Cont - CX: Sham vs. ICH: P = 0.9801, ICH vs. ICH+Vehicle: P = 0.9987, ICH+Vehicle vs. ICH+ rSEMA4C 0.15μg/kg: p = 0.7798, ICH+Vehicle vs. ICH+ rSEMA4C 0.5μg/kg:

p = 0.3543, ICH+Vehicle vs. ICH+ rSEMA4C 1.5μg/kg: p = 0.9846, Cerebellum: Sham vs. ICH: P = 0.0963, ICH vs. ICH+Vehicle: P > 0.9999, ICH+Vehicle vs. ICH+ rSEMA4C 0.15μg/kg: p > 0.9999, ICH+Vehicle vs. ICH+ rSEMA4C 0.5μg/kg:p = 0.6339, ICH+Vehicle vs. ICH+ rSEMA4C 1.5μg/kg: p = 0.5816, n = 10). All data are displayed as means ± SD, ***P < 0.001 vs. sham group, #P < 0.05 vs. ICH + Vehicle group, ###P < 0.001 vs. ICH + Vehicle group.

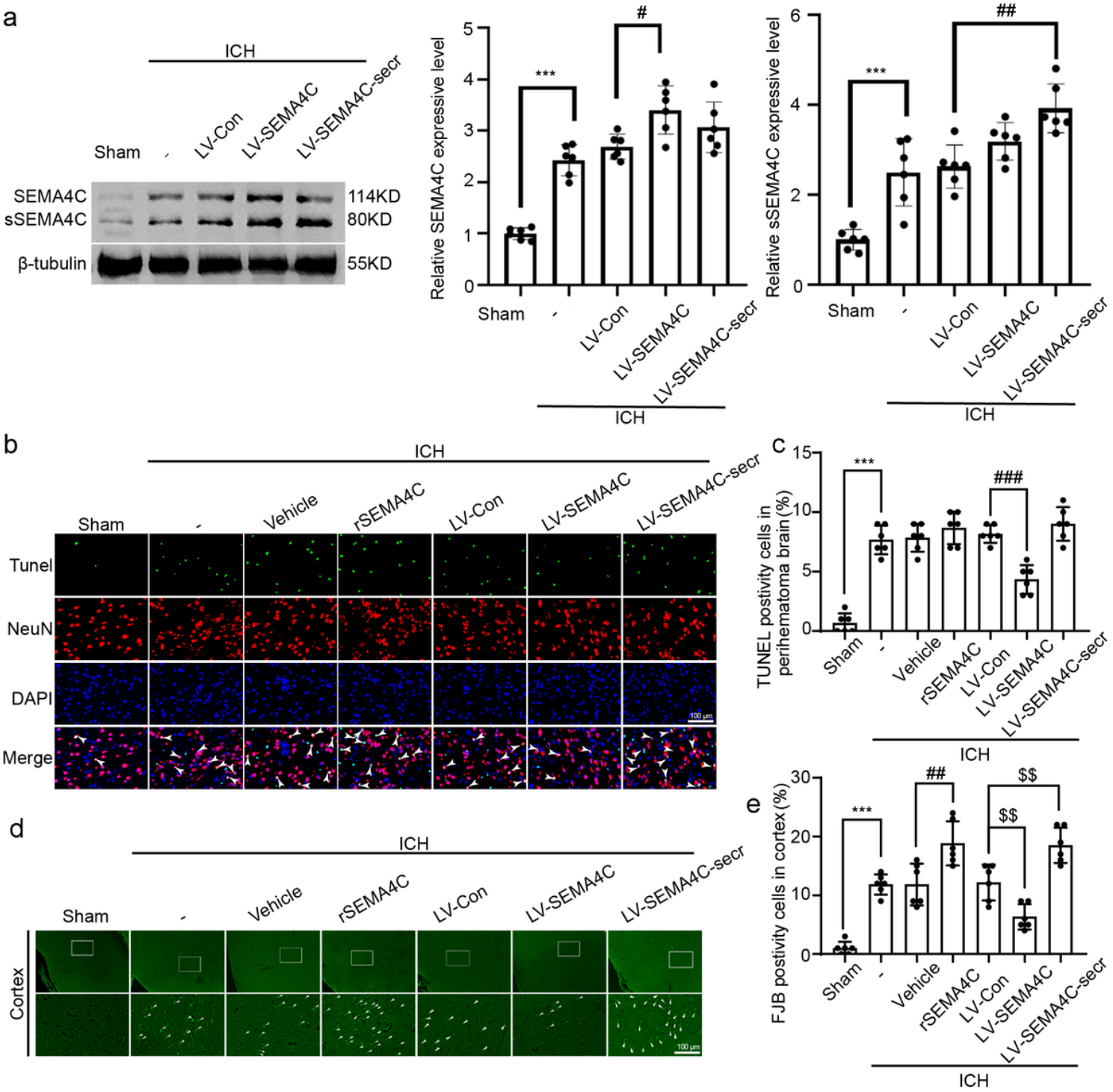

Figure 3

Effects of SEMA4C on neuronal death and degeneration in brain tissue.

(a) Western blot analysis and quantification transduction efficiency of SEMA4C (Sham vs. ICH: P < 0.0001, ICH vs. ICH + LV-Con: P = 0.7035, ICH + LV-Con vs. ICH + LV-SEMA4C: P = 0.0146, ICH + LV-Con vs. ICH + LV-SEMA4C-secr: P = 0.3657) and sSEMA4C protein level (Sham vs. ICH: P = 0.0003, ICH vs. ICH + LV-Con: P = 0.9915, ICH + LV-Con vs. ICH + LV-SEMA4C: P = 0.3544, ICH + LV-Con vs. ICH + LV-SEMA4C-secr: P = 0.0016), n = 6. (b) Double staining for TUNEL (green) neuronal maker (NeuN, red). DAPI (blue) represents the nuclei. TUNEL-positive cells are indicated by arrows; scale bar = 100 μm, n = 6. (c) Counts of TUNEL-positive cells (Sham vs. ICH: P < 0.0001, ICH vs. ICH + Vehicle: P > 0.9999, ICH + Vehicle vs. ICH + rSEMA4C: P = 0.8712, ICH vs. ICH + LV-Con: P = 0.9883, ICH + LV-Con vs. ICH + LV-SEMA4C: P < 0.0001, ICH + LV-Con vs. ICH + LV-SEMA4C-secr: P = 0.8712). (d) FJB staining of brain sections at 24 h after ICH. FJB-positive cells are indicated by arrows; scale bar = 100 μm, n = 6. (e) Counts of FJB-positive cells (Sham vs. ICH: P < 0.0001, ICH vs. ICH + Vehicle: P > 0.9999, ICH + Vehicle vs. ICH + rSEMA4C: P = 0.0092, ICH vs. ICH + LV-Con: P > 0.9999, ICH + LV-Con vs. ICH + LV-SEMA4C:P < 0.0029, ICH + LV-Con vs. ICH + LV-SEMA4C-secr: P = 0.0092). All data are presented as the mean ± SD, in a and c, ***P < 0.01 vs. sham group, #P < 0.05 vs. ICH + LV-Con group, ##P < 0.01 vs. ICH + LV-Con group, in e, ***P < 0.01 vs. sham group, ##P < 0.01 vs. ICH + Vehicle group, $$P < 0.01 vs. ICH + LV-Con group.

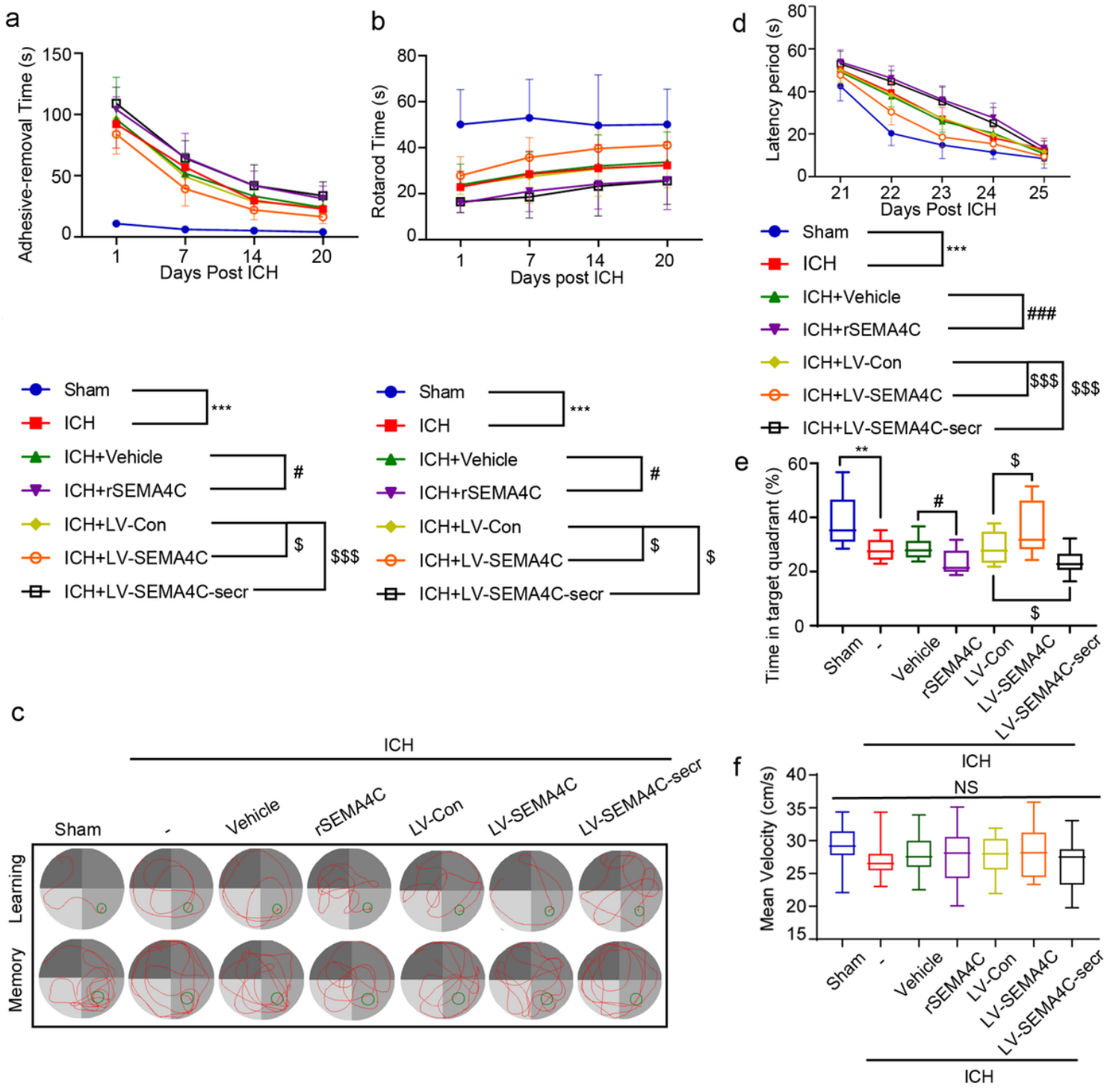

Figure 4

Effect of SEMA4C on neurological function after ICH.

(a) Adhesive-removal test (Sham vs. ICH: P < 0.0001, ICH vs. ICH + Vehicle: P > 0.9999, ICH + Vehicle vs. ICH + rSEMA4C: P = 0.0314, ICH vs. ICH + LV-Con: P > 0.9999, ICH + LV-Con vs. ICH + LV-SEMA4C: P = 0.0269, ICH + LV-Con vs. ICH + LV-SEMA4C-secr: P = 0.0006, n = 10). (b) Ratarod test (Sham vs. ICH: P < 0.0001, ICH vs. ICH + Vehicle: P > 0.9999, ICH + Vehicle vs. ICH + rSEMA4C: P = 0.0330, ICH vs. ICH + LV-

Con: P > 0.9999, ICH + LV-Con vs. ICH + LV-SEMA4C: P = 0.0481, ICH + LV-Con vs. ICH + LV-SEMA4C-secr: P = 0.0446, n = 10). (c) Representative images showing swim paths on days 23 (learning) and 26 (memory) after ICH. (d) The escape latency in the Morris water maze test at 21 to 25 days after ICH (Sham vs. ICH: P < 0.0001, ICH vs. ICH + Vehicle: P = 0.9878, ICH + Vehicle vs. ICH + rSEMA4C: P < 0.0001, ICH vs. ICH + LV-Con: P > 0.9999, ICH + LV-Con vs. ICH + LV-SEMA4C: P < 0.0001, ICH + LV-Con vs. ICH + LV-SEMA4C-secr: P = 0.0004, n = 10). (e) The time spent in the second quadrant at 26 days after ICH (Sham vs. ICH: P = 0.0029, ICH vs. ICH + Vehicle: P = 0.9801, ICH + Vehicle vs. ICH + rSEMA4C: P = 0.0326, ICH vs. ICH + LV-Con: P > 0.9999, ICH + LV-Con vs. ICH + LV-SEMA4C: P = 0.0402, ICH + LV-Con vs. ICH + LV-SEMA4C-secr: P = 0.0454, n = 10). (f) Mean swimming speed of each group in the Morris water maze test after ICH (Sham vs. ICH: P = 0.9305, ICH vs. ICH + Vehicle: P > 0.9999, ICH + Vehicle vs. ICH + rSEMA4C: P > 0.9999, ICH vs. ICH + LV-Con: P > 0.9999, ICH + LV-Con vs. ICH + LV-SEMA4C: P = 0.9997, ICH + LV-Con vs. ICH + LV-SEMA4C-secr: P = 0.9937, n = 10). All data are presented as the mean ± SD, NS: No significant difference vs. sham group, **P < 0.01 vs. sham group, ***P < 0.001 vs. sham group, #P < 0.05 vs. ICH + Vehicle, ###P < 0.001 vs. ICH + Vehicle group, $P < 0.05 vs. ICH + LV-Con group, $$$P < 0.001 vs. ICH + LV-Con group.

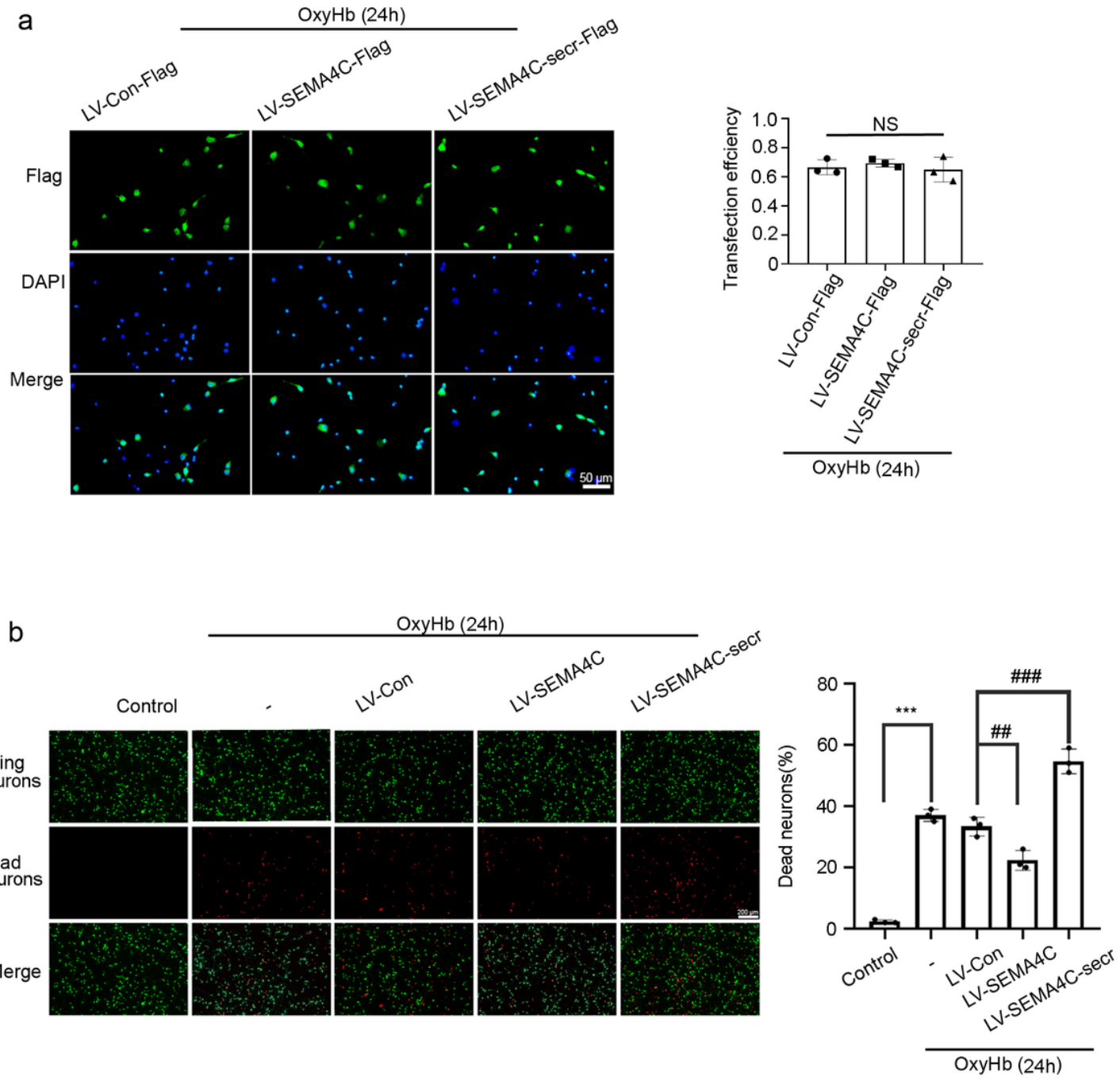

Figure 5

Transfection efficiency of SEMA4C overexpression in vitro and its effect on neuronal degeneration.

(a) Immunofluorescent staining for flag (green). Nuclei were fluorescently labeled by DAPI (blue). The diagram shows the transfection efficiency (LV-Con-Flag vs. LV-SEMA4C-Flag: P = 0.8330, LV-Con-Flag vs. LV-SEMA4C-secr-Flag: P = 0.9339, n = 3); scale bar = 50 μm. (b) Live/dead staining: green staining indicates viable cells, and red staining indicates dead cells (Control vs. OxyHb: P < 0.0001, OxyHb vs.

OxyHb + LV-Con: P = 0.5393, OxyHb + LV-Con vs. OxyHb + LV-SEMA4C: P = 0.0055, OxyHb + LV-Con vs. OxyHb + LV-SEMA4C-secr: P < 0.0001, n = 3); scale bar = 200 μm. All data are presented as the mean ± SD, NS: No significant difference vs. OxyHb + LV-Con-Flag group, ***P < 0.001 vs. control group, ##P < 0.01 vs. OxyHb + LV-Con group, ###P < 0.001 vs. OxyHb + LV-Con group.

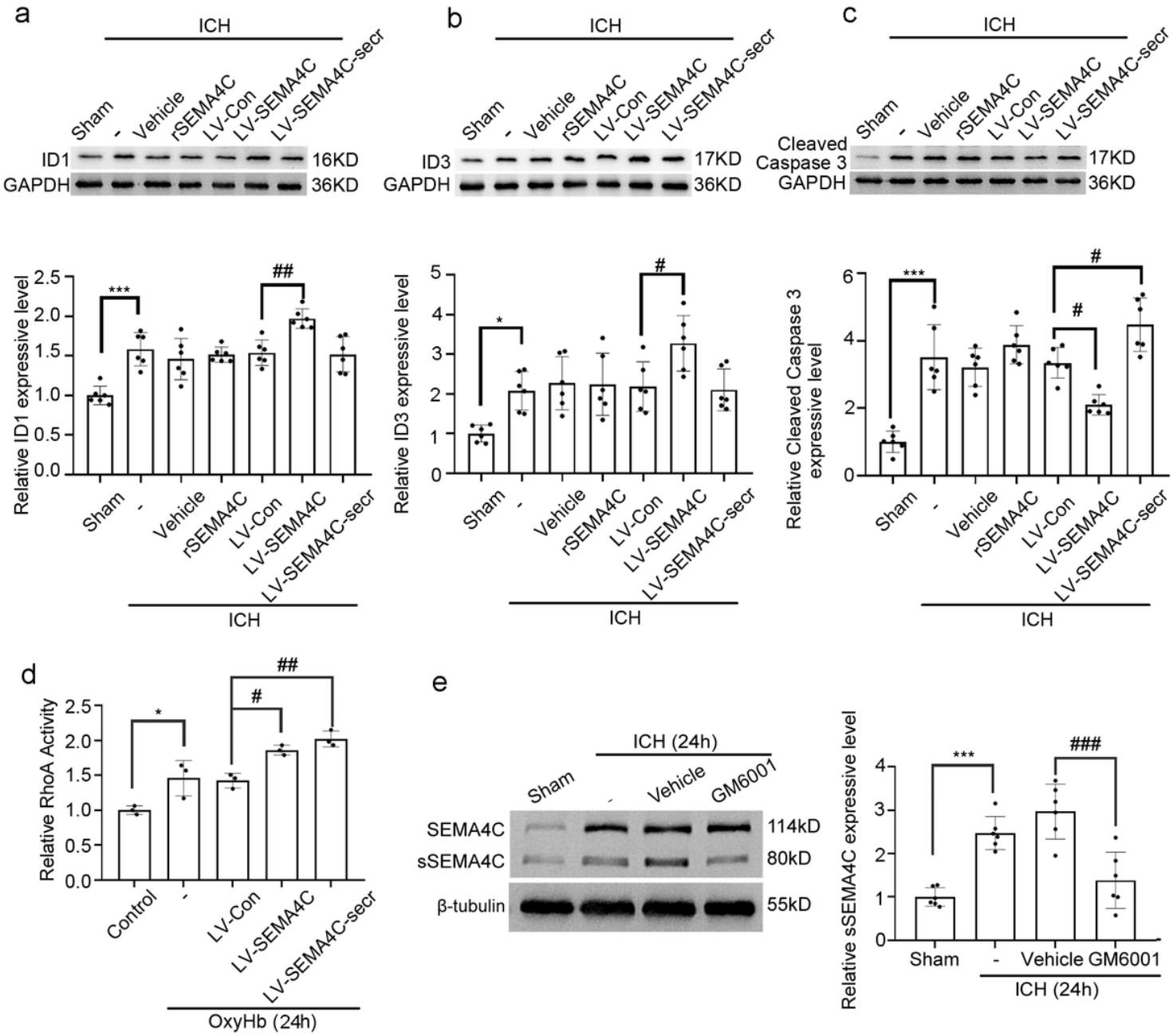

Figure 6

Roles of mSEMA4C and its cleaved form sSEMA4C in brain injury after ICH.

Western blot analysis and quantification of ID1 (a, Sham vs. ICH: P < 0.0001, ICH vs. ICH + Vehicle: P = 0.8791, ICH + Vehicle vs. ICH + rSEMA4C: P = 0.9980, ICH vs. ICH + LV-Con: P = 0.9994, ICH + LV-Con vs. ICH + LV-SEMA4C: P = 0.0033, ICH + LV-Con vs. ICH + LV-SEMA4C-secr: P > 0.9999), ID3 (b, Sham vs. ICH:

P = 0.0492, ICH vs. ICH + Vehicle: P = 0.9979, ICH + Vehicle vs. ICH + rSEMA4C: P > 0.9999, ICH vs. ICH + LV-Con: P > 0.9999, ICH + LV-Con vs. ICH + LV-SEMA4C: P = 0.0459, ICH + LV-Con vs. ICH + LV-SEMA4C-secr: P > 0.9999), and cleaved caspase-3 (c, Sham vs. ICH: P < 0.0001, ICH vs. ICH + Vehicle: P = 0.9758, ICH + Vehicle vs. ICH + rSEMA4C: P = 0.4876, ICH vs. ICH + LV-Con: P = 0.9989, ICH + LV-Con vs. ICH + LV-SEMA4C: P = 0.0183, ICH + LV-Con vs. ICH + LV-SEMA4C-secr: P = 0.0388) (n = 6). (d) Relative RhoA activity was tested by GLISA in vitro (Control vs. OxyHb: P = 0.0159, OxyHb vs. OxyHb + LV-Con: P = 0.9973, OxyHb + LV-Con vs. OxyHb + LV-SEMA4C: P = 0.0216, OxyHb + LV-Con vs. OxyHb + LV-SEMA4C-secr: P = 0.0026, n = 3). (e) Western blot analysis and quantification of effects of GM6001 on the protein level of sSEMA4C in brain tissue after ICH (Sham vs. ICH: P = 0.0003, ICH vs. ICH + Vehicle: P = 0.3518, ICH + Vehicle vs. ICH + GM6001: P = 0.0001, n = 6). All data are displayed as means ± SD; in a, b and c, *P < 0.05 vs. sham group, ***P < 0.001 vs. sham group, #P < 0.05 vs. ICH + LV-Con group, ##P < 0.01 vs. ICH + LV-Con group; in d, *P < 0.05 vs. control group, #P < 0.05 vs. OxyHb + LV-Con group, ##P < 0.01 vs. OxyHb + LV-Con group; in e, ***P < 0.001 vs. sham group, ###P < 0.001 vs. ICH + Vehicle group.

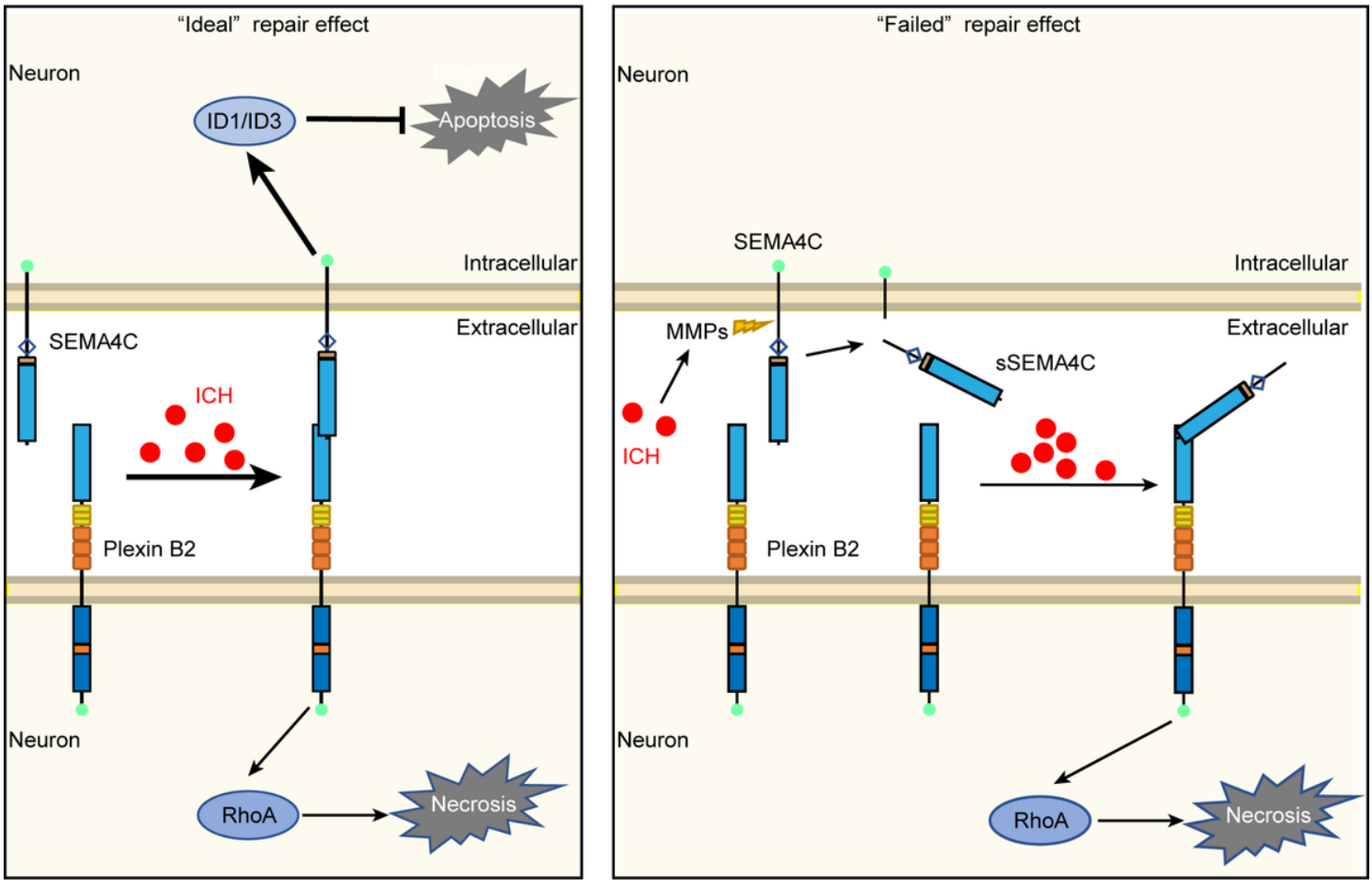

Figure 7

Potential mechanisms of SEMA4C and Plexin B2 in brain injury after ICH. After ICH, SEMA4C could interact with Plexin B2, which initiated both forward and reverse signaling. SEMA4C reverse signaling plays a dominant role and shows the "ideal" repair effect. SEMA4C are cleaved into sSEMA4C by the activation of MMPs, which failed to elicit the neuroprotective effect of SEMA4C.

Supplementary Files

This is a list of supplementary files associated with this preprint. Click to download.

- Rawdata.doc
- Supplementarymaterials.docx